Bioelectrochemistry 161 (2025) 108802

Contents lists available at ScienceDirect

Bioelectrochemistry

journal homepage: www.journals.elsevier.com/bioelectrochemistry

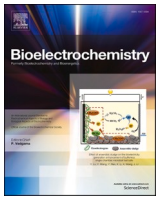

Long-term changes in transmembrane voltage after electroporation are governed by the interplay between nonselective leak current and ion channel activation

Anja Blažič [a], Manon Guinard [a], Tomaž Leskovar [a], Rodney P. O'Connor [b], Lea Rems [a,*]

[a] University of Ljubljana, Faculty of Electrical Engineering, SI-1000 Ljubljana, Slovenia
[b] Mines Saint-Etienne, Centre CMP, Département BEL, F-13541 Gardanne, France

ARTICLE INFO

Keywords:
Electroporation
Transmembrane voltage
Calcium
Temperature
Ion channels
Theoretical model

ABSTRACT

Electroporation causes a temporal increase in cell membrane permeability and leads to prolonged changes in transmembrane voltage (TMV) in both excitable and non-excitable cells. However, the mechanisms of these TMV changes remain to be fully elucidated. To this end, we monitored TMV over 30 min after exposing two different cell lines to a single 100 μs electroporation pulse using the FLIPR Membrane Potential dye. In CHO-K1 cells, which express very low levels of endogenous ion channels, membrane depolarization following pulse exposure could be explained by nonselective leak current, which persists until the membrane reseals, enabling the cells to recover their resting TMV. In U-87 MG cells, which express many different ion channels, we unexpectedly observed membrane hyperpolarization following the initial depolarization phase, but only at 33 °C and not at 25 °C. We developed a theoretical model, supported by experiments with ion channel inhibitors, which indicated that hyperpolarization could largely be attributed to the activation of calcium-activated potassium channels. Ion channel activation, coupled with changes in TMV and intracellular calcium, participates in various physiological processes, including cell proliferation, differentiation, migration, and apoptosis. Therefore, our study suggests that ion channels could present a potential target for influencing the biological response after electroporation.

1. Introduction

All cells maintain an electric potential difference across their plasma membranes, which results from the differences in membrane permeabilities for potassium, sodium, calcium and chloride ions. This potential difference is called the resting transmembrane voltage (TMV) and is maintained by a system of ion channels and pumps. In the normal physiological state, the resting TMV is negative, meaning that the cell interior is electrically more negative than its exterior. Changes in TMV have a fundamental biological function controlling the activity of various membrane proteins and act as an important biological signal closely associated with the cell cycle [1,2]. Furthermore, cells with less negative resting TMV (up to approximately −5 mV) tend to proliferate more, as observed in developing and cancerous cells [3]. Conversely, hyperpolarization (more negative TMV values, down to −90 mV) accelerates the cell differentiation process [4]. Therefore, changes in TMV can be used as an external signal to control cell proliferation, differentiation, and migration by continuous exposure (over hours) to low-intensity electric fields [1,5], a remarkable tool that is being actively explored for tissue engineering [6,7].

Long-term changes in TMV, persisting on the time scale of minutes, can also be observed after brief exposure to high-intensity pulsed electric field that result in electroporation. Electroporation is a phenomenon associated with increased plasma membrane permeability due to the creation of hydrophilic pores in the membrane lipid domains, lipid oxidation, and/or damage to certain membrane proteins, all promoted by the intense electric field [8]. Previous studies reported that electroporation is followed by prolonged membrane depolarization, lasting several minutes, both in excitable and non-excitable cells, as determined by potentiometric dyes [9] and electrophysiological measurements [10,11]. There is some evidence in the literature that these long-term changes in TMV might influence the progression of cells through the cell cycle. Electroporation with millisecond-duration electric pulses has been shown to initiate de-differentiation of cells in the limbs of newts, similar to that which occurs after limb amputation [12]. More recently, high-intensity nanosecond pulses have been shown to increase the

* Corresponding author.
E-mail address: lea.rems@fe.uni-lj.si (L. Rems).

https://doi.org/10.1016/j.bioelechem.2024.108802
Received 24 June 2024; Received in revised form 14 August 2024; Accepted 26 August 2024
Available online 30 August 2024

chondrogenic potential of mesenchymal stem cells and promote proliferation and differentiation of osteoblasts and myoblasts [13–16].

To systematically study the biological implications of long-term changes in TMV, it is of crucial importance to understand the underlying mechanisms by which electroporation alters the TMV. To this end, it is also important to establish or select an adequate methodology that allows one to monitor TMV after electroporation on a relevant time scale. While patch-clamp remains the golden standard for measuring the TMV [17], it has several limitations when it comes to electroporation research, including low throughput, perturbation of the gigaseal with high-voltage electroporation pulses and limitations on the pulse parameters that can be studied [18–20]. Another approach to measure changes in TMV is the use of voltage-sensitive fluorescent dyes. Based on their response mechanism, these dyes are divided into two classes: (i) slow-response dyes that translocate across the plasma membrane and consequently accumulate within the cells in a voltage-dependent manner, and (ii) fast-response dyes that incorporate into the membrane and have a voltage-dependent change in fluorescence emission. Fast-response dyes, such as FluoVolt and ElectroFluor630 (fluorinated version of the well-known ANEP dyes), were already used to monitor changes in action potential generation upon electroporation [21,22]. Slow-response indicators, such as the FLIPR Membrane Potential (FMP) dye, were used to detect long-term changes in TMV in excitable and non-excitable cells after exposure of cells to high-intensity pulsed electric field [9,23].

The FMP dye was originally developed for high throughput screening of ion channel activity using a plate reader [24–28]. The dye consists of two components, an anionic fluorescent voltage sensor molecule that enters the cells upon membrane depolarization and increases the cell fluorescence, and a quencher molecule that remains in the cell exterior and absorbs the fluorescence of the voltage sensor thus minimizing background fluorescence [9]. The FMP dye was demonstrated to be extremely sensitive showing a 50 % change in fluorescence per 10 mV [29]) with a large signal-to-noise ratio [30] and response time in seconds [29–31]. When compared with previously well-accepted dyes, like DiBAC4(3) [30,32–34] and dyes based on the FRET dye system [34], the FMP dye showed a greater sensitivity (response in fluorescence during membrane depolarization), a faster response time compared to DiBAC4 (3) and similar signal stability. Furthermore, an excellent correlation was shown between fluorescence changes and measurements made with the traditional patch clamp technique [29,30,33]. One of the limitations of the dye is that it can respond not only to changes in TMV at the plasma membrane but also to changes in TMV on the membranes of inner organelles [32].

Using the FMP dye, Burke et al. [23] demonstrated that prolonged membrane depolarization following pulse exposure was not solely associated with a nonselective leak current through pores in the plasma membrane, as previously thought [18,35,36]. Instead, they found that the observed depolarization may result from a more complex response involving the activation of multiple types of voltage-gated ion channels [23]. Their study exposed U-87 MG glioblastoma cells to a single 10 ns, 34 kV/cm pulse and monitored TMV changes over a 30-minute period. Inspired by this work, our primary objective was to further investigate mechanisms underlying long-term changes in TMV after exposing cells to 100 μs pulses. These longer pulses are more commonly employed in electroporation applications, including electrochemotherapy [37,38] and irreversible electroporation [39]. Following [23], we utilized the FMP dye to monitor TMV changes in U-87 MG cells, which express many different ion channels, and CHO-K1 cells, which express very low levels of endogenous ion channels. Our study delivers new insights into the mechanisms of TMV regulation after electroporation and identifies several challenges related to measuring electroporation-mediated long-term changes in TMV.

2. Materials and methods

2.1. Cell culture

Chinese hamster ovary cells (CHO-K1, #85051005) and human glioblastoma cells (U-87 MG, #9081402) were obtained from the European Collection of Authenticated Cell Cultures, Public Health England. They were grown in Ham-F12 (#N6658) and in EMEM (#51416C) medium, respectively. Both growth media were supplemented with 10 % fetal bovine serum (#F9665 for CHO-K1 and #F2442 for U-87 MG), L-glutamine (#G7513) and antibiotics (Penicillin-Streptomycin, #P0781, and Gentamicin, #G1397). All listed media and supplements were from Sigma-Aldrich, Germany. Cells were routinely passaged every 3 to 4 days, and passages between 5–30 were used for experiments. For experiments, cells were first trypsinized and counted. Afterwards 1.25×10^4 cells/3 days or 0.625×10^3 cells/4 days (CHO-K1) and 1×10^5 cells/3 days or 5×10^4 cells/4 days (U-87 MG) were seeded in Nunc Lab-Tek II chambered coverglass (Thermo Scientific™, #154461) and were grown in a humidified environment at 37 °C and 5 % CO_2.

2.2. Electric pulses

The cells were exposed to a single 100 μs electric pulse of chosen amplitude (70−630 V), delivered by a pulse generator B10 HV-LV (Leroy Biotech, France) or L-POR V0.1 (mPOR, Slovenia), through a pair of parallel Pt-Ir wire electrodes with wire diameter of 1 mm and the distance between inner edges of the electrodes of 2 mm. Delivered current and voltage were routinely monitored by the oscilloscope Wavesurfer 422, 200 MHz, the current probe CP030 and the differential probe ADP305 (all from LeCroy, USA), as per recommendations [40]. The electric field to which the cells were exposed was estimated as the ratio between the applied voltage and the interelectrode distance.

2.3. Electroporation buffer

Live Cell Imaging Solution (LCIS; Molecular Probes, #A14291DJ; composition: 140 mM NaCl, 2.5 mM KCl, 1.8 mM $CaCl_2$, 1.0 mM $MgCl_2$, 20 mM HEPES, pH 7.4, 300 mOsm), supplemented with 200 g/ml D-glucose (Gibco, #A2494001) in final 5.5 mM concentration, was selected as the electroporation buffer based on previous studies [9,23]. We did not use the growth medium for electroporation, since U-87 MG cells showed morphological changes (cell rounding and detachment) after several minutes of exposure to their growth medium (EMEM) at ambient conditions, likely due to the poor pH buffering capacity of the bicarbonate buffer at ambient CO_2 (Suppl. Material 1, Fig. S1.1a). Moreover, U-87 MG cells exhibited significantly lower cell survival when electroporated in EMEM compared with LCIS (Suppl. Material 1, Fig. S1.1b, c).

2.4. Temperature control

For experiments, the cells were first stained with selected dye (see sections 2.5-2.8), then the electrodes were positioned into the imaging chamber, and the chamber was placed on the microscope stage inside the microscope's incubator i8 Black (PeCon, Germany), as presented in Fig. 1a. Before time-lapse imaging, the cells were left for 5 min to equilibrate within the microscope's incubator. The incubator was either kept at room temperature, or at controlled temperature of 37 °C using the TempController 2000–2 (PeCon, Germany). The sample temperature was measured using a fiber optic temperature sensor (MPK-5, OpSens Solutions, Canada), see Suppl. Material 1, Fig. S1.3. At room temperature, the sample temperature was $T_{room} = 25.3 \pm 1.4$ °C (mean ± s.d.). At controlled temperature, the sample temperature was lower than 37 °C due to water evaporation from the open imaging chamber (the chamber could not be closed due to the presence of the electrodes). However, the

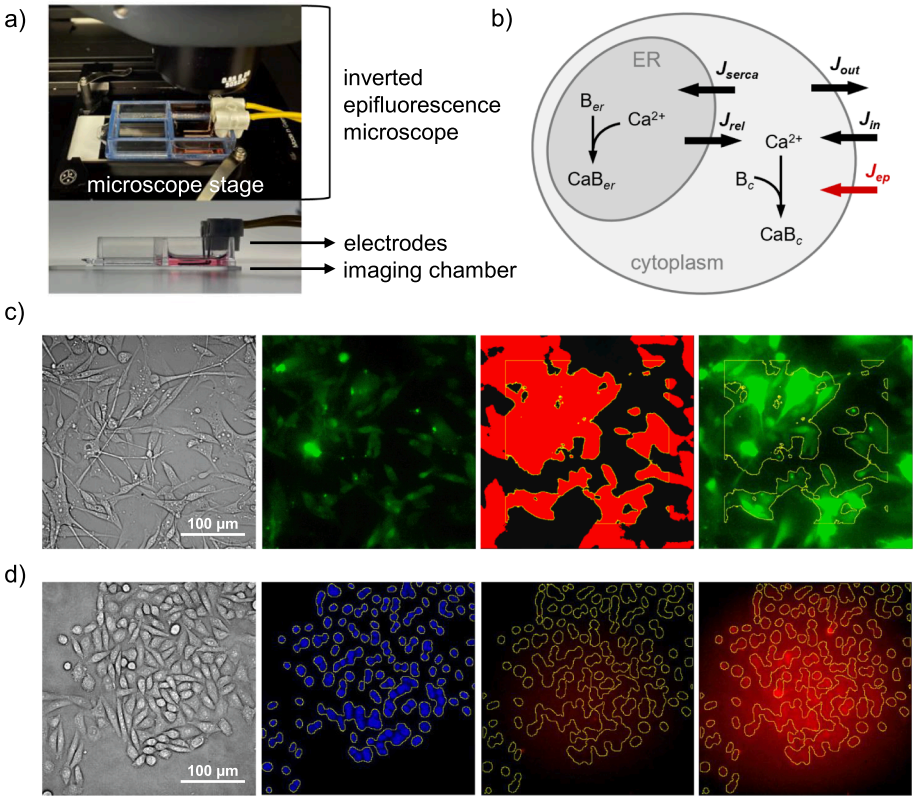

Fig. 1. Methodology. a) Experimental configuration – imaging chamber placed on the microscope stage (top) and side view of the position of electrodes within the chamber (bottom). b) Scheme of the theoretical model used to support experimental data. c) Image processing approach for determining the fluorescence of cells stained with FMP, Fluo4, and TMRE dye. An example is shown for U-87 MG cells stained with FMP dye. From left to right: brightfield image, baseline fluorescence, mask to determine the ROI corresponding to cells, maximum fluorescence reached after pulse application. d) Image processing approach for determining the fluorescence of cells stained with PI and Hoechst. Example is shown for CHO-K1 cells. From left to right: brightfield image, image of Hoechst-stained cell nuclei used to determine the ROI (yellow), baseline PI fluorescence, and PI fluorescence after pulse application at the end of 30 min time-lapse recording. Further details on the image analysis are given in Suppl. Material 2. Statistically significant differences (*: $p < 0.05$) were determined by *t*-test.

sample temperature was stable and repeatable and equal to $T_{ctrl} = 33.3 \pm 0.2$ °C.

2.5. Monitoring changes in transmembrane voltage (TMV)

For monitoring changes in TMV we used the FMP dye. FMP dye stock solution was prepared by dissolving the Component A of the FLIPR Membrane Potential Assay Red (Molecular Devices, #R7291) by adding 1 ml sterile distilled water (B.Braun, Germany) to the vial. The stock solution was mixed, aliquoted, and stored at −20 °C. To prepare the staining solution, 0.5 µL of the stock solution was dissolved in LCIS. Cells grown in the imaging chamber were stained for 30 min at 37 °C and 5 % CO_2.

Imaging was done on the Leica Thunder Imaging System with DMi8 inverted epifluorescence microscope and LED8 illumination source controlled by Las X software (all from Leica Microsystems, Germany) under 40x objective magnification. Time-lapse recordings were 30 min long, with 1 frame captured each 30 s. When monitoring the response to an electric pulse, this pulse was applied at time 1.5 min after the start of time-lapse recording. Additional brightfield and fluorescence snapshots of cells were taken before and after the time-lapse. The FMP dye was excited with green LED (554/24 nm) and its fluorescence was passed through the Leica multiband filter DFT51010 and an additional band-pass filter at 590/50 nm and detected with the Leica DFC9000 Gt camera.

The change in TMV was also measured in response to chemical depolarization by exposing cells to a mixture of 140 mM KCl and 2.5 mM NaCl, prepared by dissolving 1 M KCl (Sigma-Aldrich, #59222) and 5 M NaCl (Sigma-Aldrich, #58221) in sterile distilled water (B.Braun). After staining the cells with FMP dye, the staining solution was replaced by 125 µL of 140 mM NaCl. The imaging chamber was placed on the microscope stage and the cells were imaged at 1 frame per 5 s for 5 min. 30 s after the beginning of the time-lapse imaging, 875 µL of 160 mM KCl was added to the imaging chamber to a final concentration of 140 mM KCl. The NaCl and KCl solutions also contained the FMP dye (0.5 µL/1 ml), which ensured a consistent dye concentration, despite the change of solution.

In some experiments we also used ion channel inhibitors including, tetraethylammonium – TEA (Sigma #T2265) prepared in the sterile distilled water (B.Braun, Germany), Penitrem A (Sigma, # SI-P3053) prepared in DMSO (Sigma, #D2650), and Verapamil (Sigma, #V4629). The final concentration of ion channel inhibitors (TEA – 50 mM, Penitrem A – 2.5 µM, Verapamil – 2.2 µM) in the sample was selected following a previous study [23] and was added to the imaging chamber 5 min before commencing time-lapse imaging. The final concentration of DMSO in the sample did not exceed 1 %.

2.6. Monitoring propidium uptake

To detect changes in membrane permeability due to electroporation we used Propidium Iodide (PI; Molecular Probes, #P1304MP). To keep these experiments similar to those used for measuring the changes in TMV and intracellular calcium, which required ≥ 30 min staining steps (Sections 2.5 and 2.7, respectively), the cells were first incubated in 1 ml LCIS for 30 min at 37 °C and 5 % CO_2. The last 5 min of this incubation, we stained the cells with Hoechst 33342 (Thermo Fisher, #62249) at a

final concentration of 4 μM. Cells were washed with 1 mL LCIS and PI was added to the cells in LCIS at a final concentration of 30 μM. The cells were then handled and imaged in the same way as used for measurements with FMP dye (see Section 2.5), except for the following differences in the imaging settings: PI and Hoechst were respectively excited with green LED (554/24 nm) and violet LED (391/32 nm), and the fluorescence was passed through the DFT51010 filter with additional bandpass filter at 590/50 nm (for PI) and 460/80 nm (for Hoechst).

2.7. Monitoring intracellular calcium transients

To detect changes in intracellular calcium, cells were stained with 2 μM Fluo4-AM (Life Technologies, #F14217) in 1 ml LCIS at 37 °C and 5 % CO_2 for 45 min. For CHO-K1 cells only, we also added 2 μM Pluronic (Molecular Probes, #P3000MP) to facilitate staining. The cells were then handled and imaged in the same way as for measurements with FMP dye (see Section 2.5), except for the following differences in the imaging settings: Fluo4 was excited with blue LED (479/33 nm) and its fluorescence was passed through the DFT51010 filter with additional bandpass filter at 535/70 nm. In addition to 30 min time-lapse imaging at 1 frame per 30 s, we also captured shorter 5 min time-lapse images with faster imaging rate of 1 frame per 3 s.

After the 30 min time-lapse recordings, short-term cell survival was assessed by PI uptake, where Triton X-100 (Fluke, #93420) was used as positive control (see Suppl. Material 1, Section 2 for further details).

2.8. Monitoring changes in mitochondrial transmembrane voltage

U-87 MG cells were stained with 50 nM TMRE (Molecular Probes, #T669) in LCIS at 37 °C and 5 % CO_2 for 20 min. After staining, the cells were washed and imaged in LCIS with the same imaging settings as used with the FMP dye (see Section 2.5).

For a positive control, the proton ionophore uncoupler of oxidative respiration carbonyl cyanide 3-chlorophenylhydrazone (CCCP; Sigma-Aldrich, #C2759) was added to the TMRE-stained cells at 20 mM concentration for 5 min [41].

2.9. Image analysis

Fluorescence images were analyzed in ImageJ Fiji [42]. For FMP, Fluo4 and TMRE, the region of interest (ROI) corresponding to cells was determined based on automatic thresholding of the first image in the time-lapse sequence (Fig. 1c). For PI, the ROI corresponding to the cell nuclear area was determined based on Hoechst images captured before and after PI time-lapse, since the cells exhibited practically no baseline PI fluorescence (Fig. 1d). Further processing was the same for FMP, Fluo4, TMRE and PI. The determined ROI was applied to all images in the time-lapse to determine the mean fluorescence of the cells $F(t)$. Another ROI outside the cell region was manually selected to determine the background intensity $F_B(t)$. The change in fluorescence with time was determined as $\Delta F(t) = (F(t) - F_B(t)) - (F(t = 0) - F_B(t = 0))$. Further details on the image analysis with representative examples are provided in the Suppl. Material 2.

2.10. Statistical analysis

All results presented in the paper are based on at least three independent experimental repetitions, performed on different days. Statistical analysis was performed using SigmaPlot 11.0 (Systat Software, USA). Analysis was always carried out for each cell line separately. Baseline FMP fluorescence was compared between different temperatures (T_{room} and T_{ctrl}) using t-tests. Results of time-lapse recordings captured at different temperatures were analyzed using Two-way ANOVA (temperature and time as factors) with Holm-Sidak method for pairwise multiple comparison. Three to four time points after the start of the imaging were selected for comparison: for FMP signal at 1 min (before pulse application), 7 min (peak value), 15 min (minimum value) and 30 min (last value); for PI at 1 min and 30 min; and for Fluo4 at 1 min, 1.67 min (peak value), and 30 min (last value) for 30 min time-lapses or at 1 min, 1.65 min (peak value), and 5 min (last value) for 5 min time-lapses. Results from monitoring TMV in response to pulses with different amplitudes were analyzed with One-way ANOVA. Specifically, the minimum value of the FMP fluorescence obtained for each pulse amplitude was compared to the control condition (0 V/cm). Similarly, the maximum value of FMP fluorescence obtained for each pulse amplitude was compared to that observed using chemical depolarization.

A normality test using the Shapiro-Wilk method and equal variance test were carried out prior to conducting any specific statistical analysis. If normality and/or equal variance tests failed, nonparametric tests were performed: Mann-Whitney Rank Sum test (instead of *t*-test) and ANOVA on ranks (instead of One-way ANOVA and Two-way ANOVA). Statistically significant difference was considered for $p < 0.05$.

2.11. Theoretical modeling

For modeling the change in TMV due to electroporation, we built upon the model of Catacuzzeno et al. [43], which was originally developed to describe the role of calcium-activated potassium channels in intracellular Ca^{2+} oscillations in non-excitable cells in response to hormone stimulation. Full details of the original model and our additions, together with all model equations and parameters, are given in the Suppl. Material 3. Briefly, the model includes four relevant fluxes contributing to the intracellular Ca^{2+} dynamics (all in units of $mol{\cdot}m^{-2}{\cdot}s^{-1}$): J_{in} describes the Ca^{2+} influx through ion channels in the plasma membrane; J_{out} describes the extrusion of Ca^{2+} by plasma membrane Ca^{2+}-ATPases; J_{rel} describes the release of Ca^{2+} from the endoplasmic reticulum (ER); and J_{serca} describes the reuptake of Ca^{2+} into ER by the Ca^{2+}-ATPase SERCA. The model also includes Ca^{2+} binding to Ca^{2+} buffers (B) present in the cytoplasm and ER (Fig. 1b). We added another Ca^{2+} flux across the plasma membrane through N_{pores} with radius r_p (m) formed due to electroporation, derived based on Nernst-Planck description of electro-diffusion [44,45]:

$$J_{ep,Ca} = \frac{N_{pores}\pi {r_p}^2}{A_{pm}} D_{p,Ca} \frac{u_m + \ln(\chi)}{d_m} \frac{\chi - 1}{\ln(\chi)} \frac{[Ca]_e - [Ca]_i \exp(u_m)}{(1 - \chi \exp(u_m))} \quad (1)$$

Parameters A_{pm} (m^2) and d_m (m) are the plasma membrane area and membrane thickness, respectively; $[Ca]_e$, $[Ca]_i$ ($mol{\cdot}m^{-3}$) are the extracellular and intracellular Ca^{2+} concentrations, $D_{p,Ca}$ ($m^2{\cdot}s^{-1}$) is the diffusion coefficient of Ca^{2+} inside a pore, χ is the ratio between the extracellular and intracellular conductivity, and u_m is the non-dimensionalized TMV. The dynamic changes in TMV, denoted by U_m (V), were described by [43]

$$\frac{dU_m}{dt} = -\frac{1}{C_m}\left(g_{Ca0}(U_m - U_{Ca}) + g_{K,Ca}(U_m - U_K) + g_L(U_m - U_L) + g_{ep}U_m\right) \quad (2)$$

where C_m (F) is the plasma membrane capacitance; g_{Ca0}, $g_{K,Ca}$, and g_L (S) are the maximum conductances of calcium channels, calcium-activated potassium channels, and leak channels, respectively, whereas U_{Ca}, U_K, and U_L (V) are the reversal potentials for the corresponding ions. The last term $g_{ep}U_m$ describes the nonselective current due to electroporation, where g_{ep} (S) is the conductance of N_{pores} that reseal with the resealing function $f_{resealing}(t)$:

$$g_{ep} = N_{pores} \frac{2\sigma_p \pi {r_p}^2}{\pi r_p + 2d_m} f_{resealing}(t) \quad (3)$$

where s_p (S/m) is the effective conductivity inside the pore [46]. The resealing functions considered in the model are given later in Eqs. (4) and (5). The model was implemented and solved in Matlab R2021b

(MathWorks, USA).

3. Results and discussion

The aim of our study was to investigate the mechanisms of long-term changes in TMV after exposing CHO-K1 and U-87 MG cells to a conventional 100-μs-long electroporation pulse using the FMP dye. As we discovered that temperature affected our measurements, we first examined the influence of temperature on the baseline FMP fluorescence (Section 3.1) and on the measured cell response to an electric pulse (Section 3.2). While CHO-K1 cells responded to pulse exposure with an increase in FMP fluorescence, indicating the expected prolonged depolarization [9], U-87 MG cells kept at 33 °C unexpectedly exhibited a decrease in FMP fluorescence below baseline following the initial increase. We hypothesized that this decrease could be an artifact of FMP quencher uptake through the electroporated cell membranes. By conducting additional experiments using pulses of increasing amplitudes (Section 3.3) and employing theoretical modeling combined with experiments using ion channel inhibitors (Section 3.4), we concluded that the observed decrease in fluorescence signal is not an artifact but indicates membrane hyperpolarization due to activation of calcium-activated potassium channels. In Section 3.5, we discuss the challenges of monitoring electroporation-mediated long-term changes in TMV using the FMP dye and other dyes tested in our experiments, and propose further research directions.

3.1. FMP dye baseline fluorescence spontaneously increases at room temperature

In our preliminary experiments at room temperature (T_{room} = 25.3 ± 1.4 °C), we observed that cells stained with the FMP dye often exhibit a spontaneous increase in fluorescence over time. We hypothesized that this might be associated with non-physiological temperature, since the activity of ion channels and pumps that control the TMV decrease their activities at lower (T_{room}) temperatures [47–49]. To test this hypothesis more systematically, we controlled the temperature of the air in the incubator that surrounds the microscope stage, which resulted in sample temperature of T_{ctrl} = 33.3 ± 0.2 °C. At T_{ctrl}, the FMP fluorescence signal was stable for at least 30 min in both CHO-K1 and U-87 MG cells (Fig. 2a, red lines). In contrast, when CHO-K1 cells were imaged at T_{room}, their fluorescence gradually increased over 30 min (Fig. 2a, gray lines). Interestingly, U-87 MG cells not only exhibited a gradual increase in fluorescence at T_{room}, but were also considerably brighter at the start of the imaging. Note that we started the imaging 5 min after placing the sample on the microscope stage, to allow the temperature to equilibrate within the microscope's incubator; thus, the cells were already exposed to T_{room} (or T_{ctrl}) during this time.

To further confirm the observed increased baseline fluorescence in U-87 MG cells at T_{room}, we analyzed a larger number of CHO-K1 and U-87 MG samples. All samples were first stained at 37 °C, positioned on the microscope stage and then imaged 5 min later on the microscope, at either T_{room} or T_{ctrl}. The analysis demonstrated that the temperature significantly affected the baseline fluorescence in both CHO-K1 (*t*-test, $p < 0.001$) and U-87 MG (*t*-test, $p < 0.001$). In U-87 MG cells the baseline fluorescence was also considerably more scattered at T_{room} (Fig. 2b), reflecting greater deviations in T_{room} compared to T_{ctrl}.

3.2. The effects of temperature on the cell response to 100 μs, 1.4 kV/cm pulse: TMV, propidium uptake, and Ca^{2+} transients

The spontaneous increase in FMP fluorescence, shown in Fig. 2a, could be due to the spontaneous depolarization of cells at T_{room} or other effects of temperature on the permeation of the FMP voltage sensor molecule across the cell membrane. We explored this further by studying the effect of temperature on the response of cells to a single 100 μs, 1.4 kV/cm pulse. The chosen pulse amplitude was high enough to result in electroporation of ~40 % of both CHO-K1 and U-87 MG cells in suspension, detected through PI uptake (see Suppl. Material 1, Fig. S1.1). Note that cells attached to surfaces, as used in these experiments, electroporate at even lower electric fields than cells in suspension due to their elongated shape [50].

Changes in TMV were monitored for 30 min at T_{room} and T_{ctrl}. For both cell lines we observed that the pulse exposure triggered prolonged membrane depolarization, lasting minutes after the pulse delivery, both at T_{room} and T_{ctrl}. The maximum increase in FMP fluorescence was observed within 10 min after pulse application and was higher in both cell lines at T_{room}. The latter indicated that the FMP dye differentially stains cells at different temperatures since subsequent experiments with chemical depolarization demonstrated that both cell lines became fully depolarized at T_{ctrl} under these pulsing conditions (see Section 3.3). Furthermore, the temperature greatly influenced the recovery of the FMP signal. At T_{room}, the observed signal did not fully recover to the baseline in either of the cell lines within 30 min. This can be largely attributed to the gradual increase in the baseline FMP fluorescence (Fig. 2a); however, it is also possible that the cells were not able to fully restore their resting TMV at T_{room}. In contrast, at T_{ctrl}, the signal in CHO-K1 cells returned to its baseline ~20 min after the pulse. In U-87 MG cells, the signal even decreased below the baseline, reaching the lowest

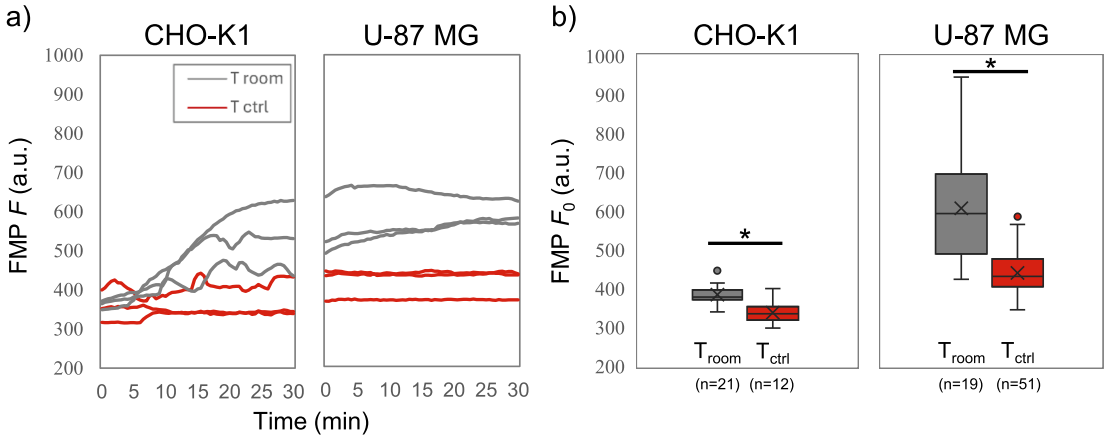

Fig. 2. Temperature-dependent stability of the baseline FMP fluorescence signal. a) Signal in CHO-K1 and U-87 MG cells on a 30-minute time scale at T_{room} (grey lines) and T_{ctrl} (red lines). b) Boxplots showing the fluorescence of CHO-K1 and U-87 MG cells, captured 5 min after placing a sample on the microscope stage at T_{room} or T_{ctrl} (this time corresponds to 0 min in panel a). Note that some of the curves for CHO-K1 in panel a) have small peaks; this was due to small spontaneous activity (small changes in TMV) of CHO-K1 cells that were not observed in U-87 MG (Suppl. Material 1, Section 4).

value 15 min after the pulse, followed by a subsequent increase towards baseline. Faster recovery of TMV at T_{ctrl} compared with T_{room} was expected due to a greater activity of ion channels and pumps that control and restore the resting TMV [47]. Nevertheless, the decrease below baseline in U-87 MG cells indicating transient membrane hyperpolarization was not expected, since previous studies reported only membrane depolarization following electroporation [9,10,10,11,23]. Statistical analysis confirmed significant differences between responses at T_{room} and T_{ctrl} at 1 min ($p = 0.010$), 15 min ($p = 0.001$) and 30 min ($p = 0.04$) in U-87 MG cells. In contrast, in CHO cells we confirmed statistically significant differences only at 1 min ($p = 0.007$) and 30 min ($p = 0.002$).

To shed more light on the difference in TMV responses between T_{room} and T_{ctrl} and between CHO-K1 and U-87 MG cells, we also monitored the time-dependent increase in membrane permeability due to electroporation using PI and keeping other conditions the same as when monitoring the changes in TMV. PI is a nucleic acid stain that can only enter cells with permeabilized membranes. In both cell lines the PI uptake was somewhat higher at T_{room} than at T_{ctrl}, but the difference was not statistically significant. U-87 MG became more brightly stained with PI than CHO-K1 at both temperatures; however, they also exhibited brighter fluorescence when permeabilized with the detergent Triton X-100 (Suppl. Material 1, Fig. S1.2), indicating a greater number of intracellular binding sites for PI (i.e. nucleic acids). To characterize the characteristic time constant of the PI uptake, we fitted the averaged data to an exponential curve, $f = A(1 - \exp(-t/\tau) + kt)$, using the function nlinfit in Matlab. For both cell lines, τ was roughly 50 % longer at T_{room} vs. T_{ctrl} (CHO-K1: $\tau = 78.5$ s vs. 53.0 s; U-87 MG: $\tau = 84.0$ s vs. 54.1 s). In both cell lines the PI curves exhibited a small but persistent increase in PI fluorescence that continued beyond the 30 min observation time. The slope k of this increase was also greater at T_{room} vs. T_{ctrl} (CHO-K1: $k = 1.87{\cdot}10^{-4}$ s^{-1} vs. $0.55{\cdot}10^{-4}$ s^{-1}; U-87 MG: $k = 1.94{\cdot}10^{-4}$ s^{-1} vs. $1.64{\cdot}10^{-4}$ s^{-1}). Both fitted parameters thus indicate slower membrane resealing kinetics at lower temperature, consistent with previous findings [51].

Since Ca^{2+} plays a crucial role in many cellular processes, we additionally monitored the changes in intracellular Ca^{2+} using the fluorescent indicator Fluo4 (Fig. 3c). Following pulse exposure, CHO-K1 cells exhibited a transient peak in intracellular Ca^{2+}, followed by a return to baseline. The peak appeared higher at T_{room} in 30 min time-lapses captured at 1 frame per 30 s. However, additional experiments using a higher imaging frame rate (1 frame per 3 s) demonstrated that the peaks were not significantly different at both T, just that the Ca^{2+} transients were faster at T_{ctrl} (Fig. 3c, inset). The full width at half maximum of the Ca^{2+} transient was ~53 s and ~34 s at T_{room} and T_{ctrl}, respectively. At T_{ctrl}, U-87 MG cells also exhibited a transient peak with full width at half maximum of ~20 s, after which the intracellular Ca^{2+} did not fully return to baseline but remained elevated almost until the end of observation time. In contrast, at T_{room}, the peak change in intracellular Ca^{2+} was much smaller. Additional experiments at higher imaging rate (1 frame per 3 s) confirmed that the Ca^{2+} transients were significantly different (1.65 min; $p = 0.05$) between T_{room} and T_{ctrl} in U-87 MG cells.

At the end of the Ca^{2+} imaging, PI was added to assess the plasma membrane integrity as an indicator of cell viability. There was no significant difference in detected PI fluorescence between T_{room} and T_{ctrl} compared to the negative control (sham-exposed cells). Moreover, the observed increase in PI fluorescence was much lower than the increase obtained after permeabilizing the cells with Triton X-100 as a positive control (Suppl. Material 1, Fig. S2.1). This confirms that most cells were able to restore their membrane integrity 30 min after pulse application.

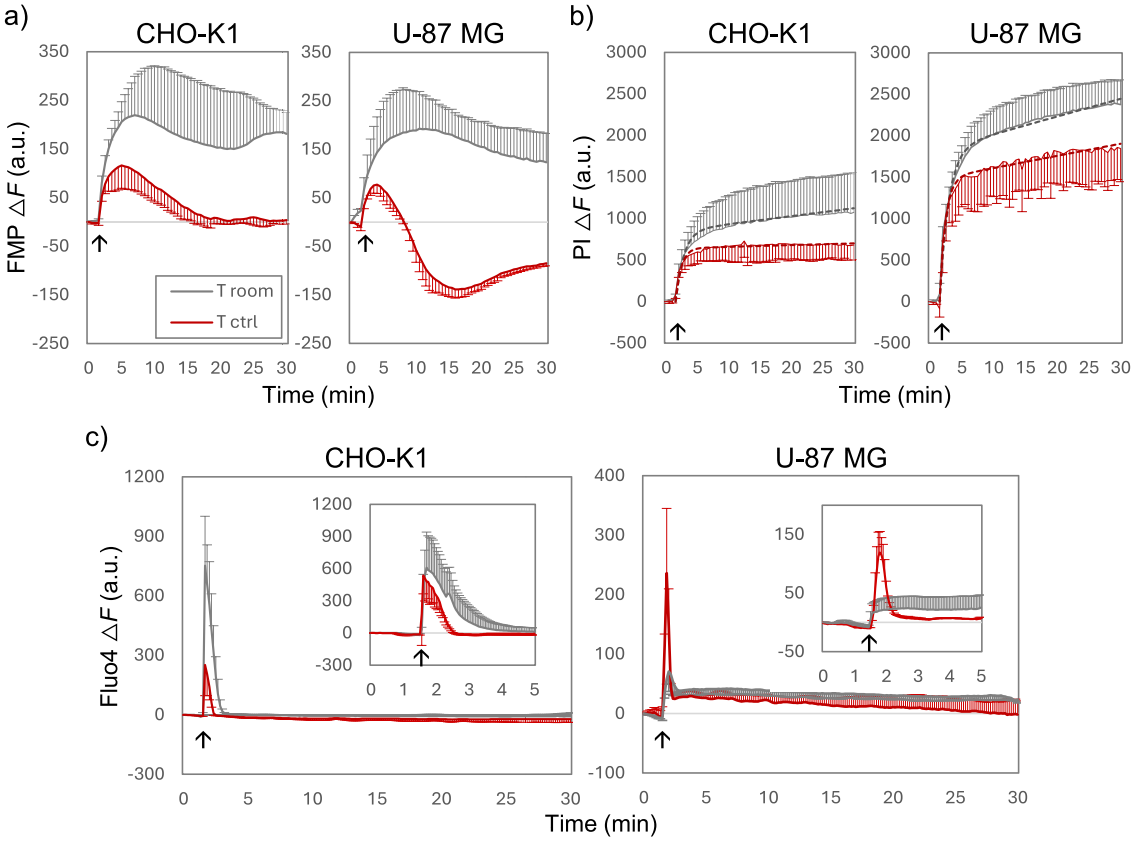

Fig. 3. The impact of temperature on the cell response after electroporation. A single 100 μs, 1.4 kV/cm pulse was delivered at 1.5 min (indicated with arrow), either at T_{room} (grey lines) or T_{ctrl} (red lines). The presented curves show mean ± s.d. from 3 to 5 experiments. Error bars are shown in one direction only for clarity. a) Response in TMV determined with FMP dye. b) Kinetics of PI uptake. The dashed curves show best fit with the function $f = A(1 - exp(-t/\tau) + kt)$. c) Calcium transients determined with Fluo4 dye. Insets show data from images captured on 5 min time scale using a higher frame rate.

However, we cannot exclude that the cells could have lost their viability later due to delayed cell death mechanisms [52,53].

3.3. Hyperpolarization of U-87 cells is not an artifact of the FMP quencher uptake

The FMP dye contains a quencher molecule that absorbs the fluorescence of the voltage sensor molecule and under physiological conditions remains on the extracellular side. However, when cells become electroporated, the quencher could potentially enter the cells. The decrease in FMP fluorescence below baseline in U-87 MG cells could thus be an artifact of quencher entry instead of membrane hyperpolarization. Furthermore, previous studies have shown that the FMP is able to indicate hyperpolarization [30] but not in all experimental conditions

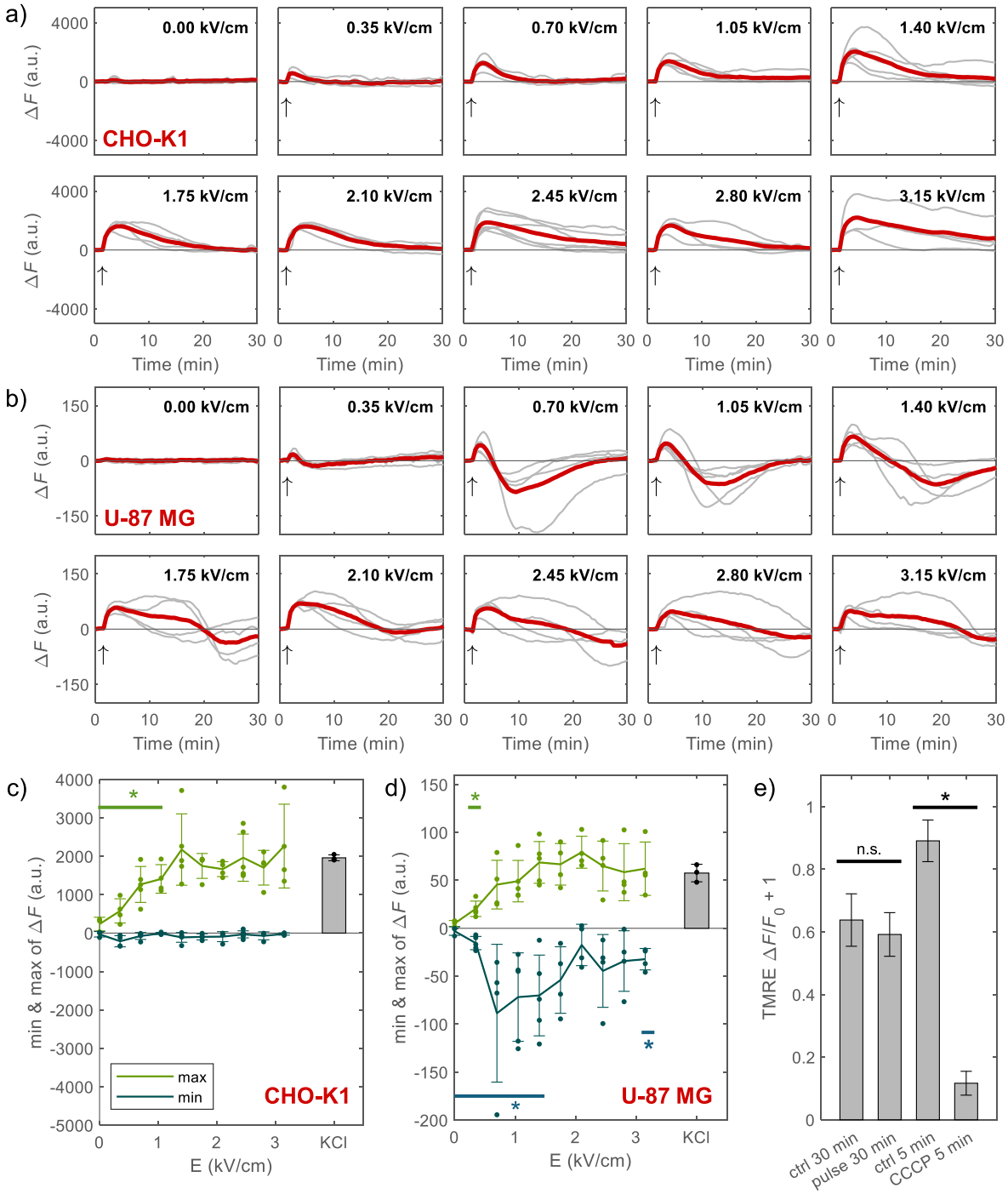

Fig. 4. Response to 100 μs pulse of different amplitudes. a) Time course of the change in FMP fluorescence in CHO-K1 cells after exposure to a pulse of a given amplitude (0 − 3.15 kV/cm). The time of pulse application is indicated with an arrow. Grey curves show responses from individual samples, obtained from at least three independent experiments; thick red curve shows their mean response. b) Same results as in a) but for U-87 MG cells. c-d) The minimum (blue lines) and maximum (green lines) values, extracted from each curve in panels a-b. Individual data points are presented together with their mean value ± standard deviation. Additionally, the bar presents the response to chemical depolarization (140 mM KCl). e) Relative change in mitochondrial TMV monitored with TMRE dye in U-87 MG cells. As a positive control for depolarization of mitochondria, the cells were exposed to CCCP for 5 min. Statistically significant differences (*: $p < 0.05$) were determined by One-way ANOVA.

[34]. To test this possibility, we exposed CHO-K1 and U-87 MG cells to a single 100 μs pulse of different amplitudes (0–3.15 kV/cm) and monitored the change in TMV over 30 min, similarly as in Fig. 3a. All experiments were performed at T_{ctrl}, since we observed a decrease in FMP fluorescence below baseline in U-87 MG cells only at this temperature.

In CHO-K1 cells, a small increase in fluorescence was already observed at 0.35 kV/cm. Pulses with amplitudes of ≥ 0.70 kV/cm all evoked similar averaged responses; the FMP signal first increased and then returned to baseline, without decreasing below baseline. In U-87 cells a small increase in fluorescence could also be observed at 0.35 kV/cm, in agreement with a previous study [9]. For amplitudes between 0.70 and 1.4 kV/cm we consistently observed an increase in fluorescence followed by a decrease below the baseline. With a further increase in pulse amplitude, this decrease below baseline became less and less profound. This indicates that the decrease below baseline is not a consequence of quencher entry since this entry should become greater with higher pulse amplitude due to a greater increase in membrane permeability.

We further extracted the minimum and maximum values from each curve in Fig. 4a, b and plotted them in Fig. 4c, d. Statistical analysis showed that the minimum values obtained after any of the pulse amplitudes applied to CHO-K1 cells were never significantly different from control. However, for U-87 MG cells, a significant difference was found at pulse amplitudes between 0.7 and 1.4 kV/cm and for 3.15 kV/cm ($p < 0.05$, shown in Fig. 4d). Additionally, we compared the extracted maximum values to chemical depolarization achieved by exposing the cells to 140 mM KCl. In CHO-K1 cells and U-87 MG cells, respectively, a significant difference ($p < 0.05$) was found compared to chemical depolarization for 0.35–1.05 kV/cm and 0.35 kV/cm. This indicates that 1.4 kV/cm pulses used in experiments presented in Fig. 3 completely depolarized the cells.

The FMP dye nonselectively stains both the plasma membrane and the membranes of intracellular organelles. Thus we hypothesized that the decrease in FMP signal below baseline in U-87 MG cells could also be due to hyperpolarization of mitochondrial membranes [54]. To detect changes in mitochondrial TMV, we used tetramethylrhodamine ethyl ester (TMRE). TMRE is a cationic dye that accumulates in active mitochondria because of the large negative TMV that appears across normal mitochondrial membranes. When the mitochondrial TMV becomes less negative (depolarizes), the TMRE concentration in the mitochondria decreases resulting in a decrease in TMRE fluorescence (the opposite of the FMP dye behavior). However, additional experiments monitoring mitochondrial TMV with TMRE dye demonstrated that mitochondria somewhat depolarized during 30 min of imaging, with or without pulse application, and were not responsible for the transient hyperpolarization observed in U-87 MG cells (Fig. 4e). To induce a depolarization of the mitochondrial TMV, CCCP was added to the cells stained with TMRE. A statistically significant difference was detected compared to the control ($p = 0.01$).

Overall, these results support the conclusion that after exposure to 100 μs pulse of intermediate amplitudes (0.7–1.4 kV/cm), the plasma membrane of U-87 MG cells first depolarized and then hyperpolarized.

3.4. Transient hyperpolarization of U-87 cells is likely caused by activation of calcium-activated potassium (K_{Ca}) channels

U-87 MG cells endogenously express calcium-activated potassium (K_{Ca}) channels [55]. These are Ca^{2+} and voltage-gated ion channels whose activation tends to hyperpolarize the membrane through the leak-out of K^+ ions along their electrochemical gradient [43]. To test the hypothesis that activation of K_{Ca} channels could be responsible for hyperpolarization, we first resorted to theoretical modeling. We used a minimal model that was originally developed to describe Ca^{2+} oscillations in hepatocytes [56] and later upgraded to include the contribution of K_{Ca} channels to these oscillations [43]. A recent review paper proposed that K_{Ca} channels play a similar role in modulating Ca^{2+} oscillations during glioblastoma cell migration and invasion [57]. We further upgraded the model to include an increase in nonselective transmembrane ionic current and Ca^{2+} uptake due to electroporation. We considered that at $t_{pulse} = 1.5$ min, when the pulse is applied, there is a certain number of pores N_{pores} created in the membrane due to electroporation. We assumed that, after the pulse exposure, the membrane reseals exponentially with a time constant $\tau = 54$ s, as determined from the fit to PI uptake kinetics in U-87 MG at T_{ctrl}:

$$f_{resealing} = \exp\left(-\frac{t - t_{pulse}}{\tau}\right), t \geq t_{pulse} \quad (4)$$

The model was able to replicate the main experimental observations. Fig. 5a shows the time course of TMV and intracellular Ca^{2+} ($[Ca^{2+}]_i$) depending on the number of pores created in the plasma membrane due to electroporation. If there are no pores created ($N_{pore} = 0$), the TMV stays at its resting value. If enough pores are created, the plasma membrane first depolarizes due to the nonselective leak current, and afterwards transiently hyperpolarizes. The simulated TMV and $[Ca^{2+}]_i$ time courses resemble well our experiments with U-87 MG cells at T_{ctrl} (see Fig. 3a,c). Note that the model shows an immediate depolarization at the time of pulse application ($t_{pulse} = 1.5$ min), whereas experimentally we see a more gradual increase in FMP fluorescence. This is because the FMP dye has a rather slow response time in seconds [29–31]. Studies using potentiometric dyes with fast response indeed demonstrate an immediate step-like depolarization following application of an electroporating pulse [21].

Membrane hyperpolarization in the model is due to activation of K_{Ca} channels, as demonstrated in Fig. 5b, which shows the TMV and $[Ca^{2+}]_i$, depending on the maximum conductance of K_{Ca} channels, when $N_{pore} = 1000$. Without K_{Ca} channels ($g_{Kmax} = 0$ nS), the plasma membrane transiently depolarizes and returns to baseline without any hyperpolarization. This TMV time course resembles that of CHO-K1 cells that express very low levels of endogenous ion channels [58,59] (see Fig. 3a). With increasing levels of expressed K_{Ca} channels, transient hyperpolarization becomes more profound. On the contrary, the time course of $[Ca^{2+}]_i$ is not affected much by K_{Ca} channels, consistent with qualitatively similar Ca^{2+} transients in CHO-K1 and U-87 MG cells observed experimentally at T_{ctrl} (see Fig. 3c).

It is important to emphasize that while the plasma membrane is highly permeable in the first few minutes after the pulse, the nonselective leak current is so high that activation of K_{Ca} channels does not affect the TMV very much. However, as the membrane mostly reseals and the leak current becomes very small, ion channel activation can have a large influence on the restoration of TMV. To illustrate this point, we assumed that a certain fraction δ of pores or permeable defects can persist in the membrane even after completion of the exponential resealing phase characterized by time τ. The presence of such pores can explain the small linear increase in the PI uptake that persisted until the end of observation time (Fig. 3b). The corresponding resealing function is:

$$f_{resealing} = (1 - \delta)\exp\left(-\frac{t - t_{pulse}}{\tau}\right) + \delta, t \geq t_{pulse} \quad (5)$$

The parameter δ is related to the slope k, extracted from the fit to PI uptake curves in Fig. 3b (see Suppl. Material 3 for derivation):

$$\delta = \frac{k\tau}{1 + k\tau} \quad (6)$$

For easier comparison with experiments, we thus varied the value of the slope k. The calculations are presented in Fig. 5c. If k is smaller than a certain value, the TMV response shows both the initial depolarization and the subsequent hyperpolarization. However, with increasing k, the membrane only depolarizes after the pulse. To further explore the conditions in which hyperpolarization can be observed, we made a parametric analysis in which we varied N_{pore} and k, and for each parameter combination we determined the minimum TMV that was

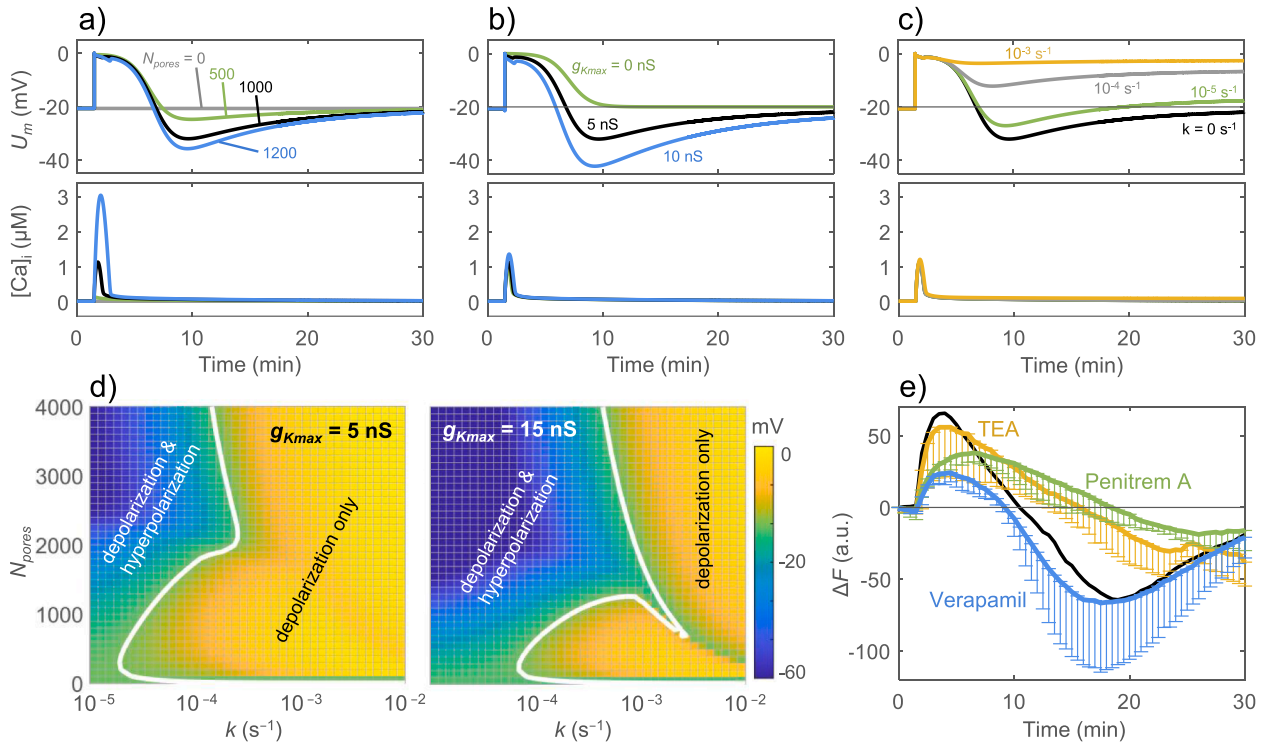

Fig. 5. The influence of K_{Ca} channels on TMV after electroporation. a-c) Time course of TMV and $[Ca^{2+}]_i$ predicted from the theoretical model for different values of model parameters; a) Results for different number of pores N_{pore}, when the maximum conductance of K_{Ca} channels equals $g_{Kmax} = 5$ nS and the parameter $k = 0$ s^{-1}. The pores are created when the pulse is applied at $t_{pulse} = 1.5$ min. b) Similar results as in a), but for different values of g_{Kmax} when $N_{pore} = 1000$ and $k = 0$ s^{-1}. c) Similar results as in a), but for different values of parameter k when $g_{Kmax} = 5$ nS and $N_{pore} = 1000$. d) Parametric analysis showing the minimum TMV value obtained in the model within 30 min after the pulse, depending on parameters k and N_{pore}. Calculations were performed for $g_{Kmax} = 5$ nS (left) and 50 nS (right). e) Experimental measurements of the change in TMV after exposure to 100 ms, 1.4 kV/cm at $t_{pulse} = 1.5$ min in U-87 MG cells with the FMP dye in the presence of ion channel inhibitors TEA, Penitrem A, and Verapamil. Mean ± s.d. from 3 independent experiments. The thin black line shows the average response without ion channel inhibitors, taken from Fig. 4b at 1.4 kV/cm.

achieved within 30 min after the pulse. We performed the parametric analysis for two values of the maximum conductance of K_{Ca} channels ($g_{Kmax} = 5$ nS and 15 nS), since we did not find an exact value of g_{Kmax} for U-87 MG cells in the literature. The results are presented in Fig. 5d. The white line separates the parameter space in which both depolarization and hyperpolarization can be observed, from the space where only depolarization can be observed after the pulse. The graphs clearly show that hyperpolarization occurs only when k is sufficiently small to be on the left side of the white line. When there are more K_{Ca} expressed in the cells (g_{Kmax} is larger), the white line shifts to larger k.

The parametric analysis additionally elucidates our experimental results. Experimentally, hyperpolarization in U-87 MG cells became less profound with increasing pulse amplitude. The model suggests this is not due to more pores created by a pulse with higher amplitude but to slower or incomplete membrane resealing. Furthermore, we found a greater slope k in PI uptake kinetics at T_{room} compared to T_{ctrl}. Thus, the absence of hyperpolarization in U-87 MG cells at T_{room} could partially be due to a larger k. Even more importantly, at T_{room}, the increase in $[Ca^{2+}]_i$ in U-87 MG cells was significantly lower than at T_{ctrl}. The increase in $[Ca^{2+}]_i$ at T_{room} was likely too low to activate K_{Ca} channels (see the influence of $[Ca^{2+}]_i$ peak amplitude on the extent of hyperpolarization in Fig. 5a). However, the model in the current form was unable to represent the altered $[Ca^{2+}]_i$ profile at T_{room}, thus further research is needed to fully understand the absence of hyperpolarization in U-87 MG cells at T_{room}. Overall, our model confirms that the observed hyperpolarization in U-87 MG cells can be due to the activation of K_{Ca} channels.

The modeling predictions were supported by experiments using ion channel inhibitors. A nonspecific inhibitor of potassium channels TEA, in concentrations high enough to inhibit both large conductance (BK) and intermediate conductance (IK) calcium-activated potassium channels, abrogated hyperpolarization (Fig. 5e). Additional experiments with the BK inhibitor Penitrem A resulted in similar responses as with TEA, suggesting that hyperpolarization is mainly governed by the activation of BK channels. The minimum FMP fluorescence values in the presence of both TEA and Penitrem A were significantly different from control without ion channel inhibitors (Two-way ANOVA, $p \leq 0.03$). On the contrary, the inhibitor of voltage-gated calcium channels Verapamil did not have a significant effect on hyperpolarization. This is to some extent consistent with our assumption in the model that the increase in $[Ca^{2+}]_i$ after the pulse is mainly due to influx of Ca^{2+} through pores in the membrane, rather than activation of Ca^{2+} channels. Nevertheless, while the maximum FMP fluorescence value with TEA and Penitrem A was not significantly different from control, it was significantly lower with Verapamil (Two-way ANOVA, $p = 0.016$). This indicates that calcium channel activation can also contribute to the initial depolarization phase. It should be noted that U-87 MG cells express many different types of ion channels; addition of these channels to the model would likely further improve the agreement with experiment.

Overall, our model and experiments demonstrate that the observed long-term changes in TMV in U-87 MG cells can be explained by the dynamic interplay between the nonselective leak current due to electroporation and ion channel activation. The nonselective leak current acts to depolarize the TMV towards 0 mV, whereas ion channel activation influences the TMV when the nonselective leak current becomes very small and comparable to the currents passing through ion channels. The previous study by Burke et al. on U-87 MG cells exposed cells to a 10 ns, 34 kV/cm pulse demonstrated that immediately after the pulse application, the activation of Ca^{2+}, BK and TRPM8 ion channels contributes to membrane depolarization [23]. The pulse amplitude used in this study was just above the threshold for inducing membrane

depolarization and was thus probably associated with a very small increase in membrane permeability and leak current – small enough to enable the ion channel currents to influence the TMV. Our results indicate that after exposing cells to 100 μs, 1.4 kV/cm pulse, membrane depolarization is mainly associated with the nonselective leak current due to increased membrane permeability. Nevertheless, the lower amplitude of depolarization detected in the presence of Verapamil suggests that activation of calcium channels can to some extent contribute to the initial depolarization phase as well.

3.5. Challenges associated with monitoring long-term TMV changes after electroporation

Both our model and experiments with ion channel inhibitors confirm that the decrease in FMP fluorescence below baseline, observed in U-87 MG cells following pulse exposure, can be attributed to plasma membrane hyperpolarization. We nevertheless wanted to additionally confirm this with two alternative voltage-sensitive dyes, ElectroFluor630 and FluoVolt. Both have already been used for monitoring TMV changes in response to high-voltage electric pulses; however, they were previously only used to detect short-term changes, i.e. in the range of seconds [21,22].

Our results, presented in Suppl. Material 1 Section 5, together with a detailed explanation of the dyes, reveal considerable limitations of both dyes. With ElectroFluor630 we observed the well-known gradual internalization of the dye. While this internalization is not necessarily problematic for monitoring rapid TMV changes (such as action potentials) [21,60], it makes it very challenging to monitor long-term and small changes in TMV over a 30 min observation period, since the fluorescence signal continuously drifts. Further limitations of the dye are photobleaching and a rather low sensitivity (~15 % / 100 mV) [61], which for U-87 MG cells with a mean resting voltage of − 16 ± 4 mV [55] requires detection of fluorescence changes below 2.4 %. With FluoVolt, we observed morphological changes and cell rounding over the 30 min period, which we attributed to phototoxicity, as previously reported [62]. Therefore, we found ElectroFluor630 and FluoVolt unsuitable for monitoring long-term changes in TMV after electroporation in our experimental setup. The FMP dye was considered superior for our experimental study.

Nevertheless, FMP dye also has limitations. It was designed for measurements of intact plasma membranes. During electroporation both parts of the dye (the anionic voltage sensor molecule and the quencher molecule) could potentially enter the cell due to increased membrane permeability and influence the fluorescence signal. Our experiments with pulses of different amplitudes (up to 3.15 kV/cm) showed that quencher entry was not critical under our specific pulsing conditions. However, we cannot exclude that other pulse parameters, associated with a greater increase in membrane permeability, would allow the quencher to enter the cells. Another problem impeding the interpretation of results is the unknown chemical structure of both the voltage sensor and quencher molecule, which is considered proprietary information.

It is further interesting to note that our results with the FMP dye became less reproducible for pulses with the highest tested amplitudes (Fig. 4a-b). For pulse amplitudes higher than 1.4 kV/cm, both CHO-K1 and U87-MG cells started to fuse due to electroporation – a phenomenon known as electrofusion [63] – which could be the one of the reasons for lower reproducibility. Moreover, higher pulse amplitude is associated with stronger electroporation and thus greater structural changes of the membrane, which could affect the translocation mechanism of the FMP voltage sensor molecule.

Overall, we find that measuring long-term changes in TMV remains challenging in electroporation research from the methodological point of view and that all the tested dyes (FMP, ElectroFluor630 and FluoVolt) have limitations. A promising alternative could be genetically encoded voltage indicators (GEVIs), which have not yet been experimentally tested when used for observations of the TMV following delivery of high-intensity electric pulses. Nevertheless, one of their limitations is a possible perturbation of the protein voltage sensor domain by a strong electric field, which was already shown in molecular dynamics simulations of voltage-dependent calcium and sodium channels [64,65]. Moreover, all GEVIs require cell transfection, which can perturb the wild-type cell physiology [66].

4. Conclusions and outlook

In our study we investigated the mechanisms of long-term changes in TMV after exposing CHO-K1 and U-87 MG cells to a single 100 μs electroporation pulse. By monitoring changes in TMV over a period of 30 min with the FMP dye, we observed that these changes are cell type and temperature dependent. In CHO-K1 cells, which express low levels of endogenous ion channels, membrane depolarization following pulse exposure could mainly be explained by the nonselective leak current through the permeabilized membrane, which persists until the membrane reseals, enabling the cells to recover their resting TMV. Membrane resealing and TMV recovery was faster at higher (33 °C), more physiological, temperature compared with experiments performed at room temperature (25 °C). U-87 MG cells, which express many endogenous ion channels, exhibited a different response in TMV than CHO-K1. Following the initial depolarization phase, the cells hyperpolarized, but only at 33 °C. Using a theoretical model, supported by experiments with ion channel inhibitors, we found that this hyperpolarization can largely be attributed to the activation of calcium-activated potassium (K_{Ca}) channels. However, since we were unable to completely abrogate hyperpolarization with selected K_{Ca} channel inhibitors, activation of other channels, such as chloride channels could contribute as well [67]. Based on the obtained experimental and theoretical results, we conclude that as long as the membrane is highly permeable, the nonselective leak current is responsible for membrane depolarization. However, when the leak current becomes comparable to the currents through ion channels (towards the end of the membrane resealing phase or when the membrane is only gently electroporated), ion channel activation can significantly contribute to the changes in TMV.

TMV is known to change through the progression of the cell cycle [1]. The TMV controls the activation of voltage-gated ion channels and modulates the function of other membrane proteins exhibiting voltage sensitivity [68]. Since many of these channels conduct calcium ions, changes in TMV affect the intracellular calcium levels and calcium signaling. Ion channels are abundantly expressed in cancer cells including glioblastoma, from which the U-87 MG cell line derives [55]. It was demonstrated that ion channels have an important role in cancer cell proliferation, migration, invasion, and apoptosis, which led to proposition of classifying cancer as one of channelopathies [69,70]. Therefore, ion channels are considered as therapeutic targets for cancer treatment. A recent study in glioblastoma cell lines NG108-15 and U-87 MG confirmed that certain combinations of ion channel modulating drugs significantly reduce proliferation, make the cells senescent, and promote differentiation [71]. Our study demonstrated that electroporation provokes a dynamic change in TMV in U-87 MG cells, which modulates ion channel activation. It would therefore be interesting to study the functional consequences of such changes in TMV and how they affect cell behavior. Such studies would provide new insights into electroporation-based treatments of glioblastoma and other cancers [38,72,73]. Since we found that changes in TMV are temperature-dependent, such studies should ensure controlled temperature conditions, ideally physiological conditions at 37 °C.

To further study long-terms changes in TMV following electroporation, one needs to establish a reliable methodology. While the fast-response voltage-sensitive dyes FluoVolt and ElectroFluor630 were previously used to monitor short-term changes in TMV (time scale of a few seconds) following electroporation [21,22], we found them unsuitable for monitoring long-term TMV changes. The slow-response FMP

dye was better suited for this purpose, although here we also identified several limitations when using the dye in combination with electroporation. Voltage-sensitive dyes are generally designed and calibrated based on experiments made with intact membranes. However, when a cell is electroporated, both the increase in membrane permeability and the perturbations of the membrane structure could potentially interfere with the function of the dye and alter the fluorescence signal. Moreover, for electroporation research, it would be important to test voltage-sensitive dyes in electroporated cells using classical electrophysiological (patch clamp) measurements. Further research should also be focused on developing better methods for monitoring long-term changes in TMV following electroporation. Novel genetically encoded voltage indicators (GEVIs) could present a promising tool [66], provided that the electric field used for electroporation does not damage the GEVI's voltage-sensor domains [65].

CRediT authorship contribution statement

Anja Blažič: Writing – review & editing, Writing – original draft, Visualization, Methodology, Investigation, Formal analysis, Data curation, Conceptualization, Validation. **Manon Guinard:** Writing – review & editing, Methodology, Investigation, Validation. **Tomaž Leskovar:** Writing – review & editing, Methodology, Investigation, Software, Validation. **Rodney P. O'Connor:** Writing – review & editing, Methodology, Conceptualization. **Lea Rems:** Writing – review & editing, Writing – original draft, Supervision, Project administration, Methodology, Funding acquisition, Formal analysis, Conceptualization, Resources, Software, Validation, Visualization.

Declaration of competing interest

The authors declare that they have no known competing financial interests or personal relationships that could have appeared to influence the work reported in this paper.

Data availability

Data will be made available on request.

Acknowledgments

The study was supported by funding from the European Union's Horizon 2020 research and innovation programme under the Marie Skłodowska-Curie grant agreement No. 893077 (to L.R.), Erasmus + programme (to M.G. and A.B.), and by the Slovenian Research and Innovation Agency (ARIS) within research programme P2-0249, research projects J2-2503 and MN-0023, infrastructure programme I0-0022, and funding for Junior Researchers. The work was in part supported by the European Union and ARIS through NextGenerationEU and NOO funding within project MN-0023. The study was also partially supported by ARIS and the University of Ljubljana within the funding for Start-up Research Programme, and by the European Union's Horizon Europe research and innovation programme within the ERC Starting Grant project No. 101115323 – REINCARNATION. Views and opinions expressed are however those of the author(s) only and do not necessarily reflect those of the European Union or the European Research Council. Neither the European Union nor the granting authority can be held responsible for them. The authors thank Tina Cimperman for initial help with analysis of the FMP dye signals, Tina Batista Napotnik for help with experiments with the ElectroFluor630 dye, Simon Žakelj for preparing Verapamil stock solution, and Damijan Miklavčič for useful comments to the manuscript.

Appendix A. Supplementary data

Supplementary data to this article can be found online at https://doi.org/10.1016/j.bioelechem.2024.108802.

References

[1] D.J. Blackiston, K.A. McLaughlin, M. Levin, Bioelectric controls of cell proliferation: ion channels, membrane voltage and the cell cycle, Cell Cycle Georget. Tex 8 (2009) 3527–3536, https://doi.org/10.4161/cc.8.21.9888.
[2] H.G. Sachs, P.J. Stambrook, J.D. Ebert, Changes in membrane potential during the cell cycle, Exp. Cell Res. 83 (1974) 362–366, https://doi.org/10.1016/0014-4827(74)90350-4.
[3] M. Yang, W.J. Brackenbury, Membrane potential and cancer progression, Front. Physiol. 4 (2013) 185, https://doi.org/10.3389/fphys.2013.00185.
[4] S. Sundelacruz, M. Levin, D.L. Kaplan, Role of Membrane Potential in the Regulation of Cell Proliferation and Differentiation, Stem Cell Rev. Rep. 5 (2009) 231–246, https://doi.org/10.1007/s12015-009-9080-2.
[5] L. Vodovnik, D. Miklavčič, G. Serša, Modified cell proliferation due to electrical currents, Med. Biol. Eng. Comput. 30 (1992) CE21–CE28, https://doi.org/10.1007/BF02446174.
[6] G. Thrivikraman, S.K. Boda, B. Basu, Unraveling the mechanistic effects of electric field stimulation towards directing stem cell fate and function: a tissue engineering perspective, Biomaterials 150 (2018) 60–86, https://doi.org/10.1016/j.biomaterials.2017.10.003.
[7] L. Leppik, K.M.C. Oliveira, M.B. Bhavsar, J.H. Barker, Electrical stimulation in bone tissue engineering treatments, Eur. J. Trauma Emerg. Surg. off. Publ. Eur. Trauma Soc. 46 (2020) 231–244, https://doi.org/10.1007/s00068-020-01324-1.
[8] T. Kotnik, L. Rems, M. Tarek, D. Miklavčič, Membrane electroporation and electropermeabilization: mechanisms and models, Annu. Rev. Biophys. 48 (2019) 63–91, https://doi.org/10.1146/annurev-biophys-052118-115451.
[9] J. Dermol-Černe, D. Miklavčič, M. Reberšek, P. Mekuč, S.M. Bardet, R. Burke, D. Arnaud-Cormos, P. Leveque, R. O'Connor, Plasma membrane depolarization and permeabilization due to electric pulses in cell lines of different excitability, Bioelectrochemistry Amst. Neth. 122 (2018) 103–114, https://doi.org/10.1016/j.bioelechem.2018.03.011.
[10] A.G. Pakhomov, R. Shevin, J.A. White, J.F. Kolb, O.N. Pakhomova, R.P. Joshi, K. H. Schoenbach, Membrane permeabilization and cell damage by ultrashort electric field shocks, Arch. Biochem. Biophys. 465 (2007) 109–118, https://doi.org/10.1016/j.abb.2007.05.003.
[11] M. Neunlist, L. Tung, Dose-dependent reduction of cardiac transmembrane potential by high-intensity electrical shocks, Am. J. Physiol. 273 (1997) H2817–H2825, https://doi.org/10.1152/ajpheart.1997.273.6.H2817.
[12] D.L. Atkinson, T.J. Stevenson, E.J. Park, M.D. Riedy, B. Milash, S.J. Odelberg, Cellular electroporation induces dedifferentiation in intact newt limbs, Dev. Biol. 299 (2006) 257–271, https://doi.org/10.1016/j.ydbio.2006.07.027.
[13] R.A. Vadlamani, Y. Nie, D.A. Detwiler, A. Dhanabal, A.M. Kraft, S. Kuang, T. P. Gavin, A.L. Garner, Nanosecond pulsed electric field induced proliferation and differentiation of osteoblasts and myoblasts, J. r. Soc. Interface 16 (2019) 20190079, https://doi.org/10.1098/rsif.2019.0079.
[14] T. Ning, J. Guo, K. Zhang, K. Li, J. Zhang, Z. Yang, Z. Ge, Nanosecond pulsed electric fields enhanced chondrogenic potential of mesenchymal stem cells via JNK/CREB-STAT3 signaling pathway, Stem Cell Res. Ther. 10 (2019) 45, https://doi.org/10.1186/s13287-019-1133-0.
[15] J. Chen, Y. Huang, J. Yang, K. Li, Y. Jiang, B.C. Heng, Q. Cai, J. Zhang, Z. Ge, Multiple nanosecond pulsed electric fields stimulation with conductive poly(l-lactic acid)/carbon nanotubes films maintains the multipotency of mesenchymal stem cells during prolonged in vitro culture, J. Tissue Eng. Regen. Med. 14 (2020) 1136–1148, https://doi.org/10.1002/term.3088.
[16] A. Halim, A.D. Ariyanti, Q. Luo, G. Song, Recent progress in engineering mesenchymal stem cell differentiation, Stem Cell Rev. Rep. 16 (2020) 661–674, https://doi.org/10.1007/s12015-020-09979-4.
[17] P. Liu, E.W. Miller, Electrophysiology, Unplugged: Imaging Membrane Potential with Fluorescent Indicators, Acc. Chem. Res. 53 (2020) 11–19, https://doi.org/10.1021/acs.accounts.9b00514.
[18] A.G. Pakhomov, J.F. Kolb, J.A. White, R.P. Joshi, S. Xiao, K.H. Schoenbach, Long-lasting plasma membrane permeabilization in mammalian cells by nanosecond pulsed electric field (nsPEF), Bioelectromagnetics 28 (2007) 655–663, https://doi.org/10.1002/bem.20354.
[19] L.H. Wegner, W. Frey, A. Silve, Electroporation of DC-3F Cells Is a Dual Process, Biophys. J. 108 (2015) 1660–1671, https://doi.org/10.1016/j.bpj.2015.01.038.
[20] A.G. Pakhomov, A.M. Bowman, B.L. Ibey, F.M. Andre, O.N. Pakhomova, K. H. Schoenbach, Lipid nanopores can form a stable, ion channel-like conduction pathway in cell membrane, Biochem. Biophys. Res. Commun. 385 (2009) 181–186, https://doi.org/10.1016/j.bbrc.2009.05.035.
[21] T. Batista Napotnik, B. Kos, T. Jarm, D. Miklavčič, R.P. O'Connor, L. Rems, Genetically engineered HEK cells as a valuable tool for studying electroporation in excitable cells, Sci. Rep. 14 (2024) 720, https://doi.org/10.1038/s41598-023-51073-5.
[22] A.G. Pakhomov, I. Semenov, M. Casciola, S. Xiao, Neuronal excitation and permeabilization by 200-ns pulsed electric field: an optical membrane potential study with FluoVolt dye, Biochim. Biophys. Acta Biomembr. 2017 (1859) 1273–1281, https://doi.org/10.1016/j.bbamem.2017.04.016.
[23] R.C. Burke, S.M. Bardet, L. Carr, S. Romanenko, D. Arnaud-Cormos, P. Leveque, R. P. O'Connor, Nanosecond pulsed electric fields depolarize transmembrane potential via voltage-gated K+, Ca2+ and TRPM8 channels in U87 glioblastoma cells, Biochim. Biophys. Acta Biomembr. 2017 (1859) 2040–2050, https://doi.org/10.1016/j.bbamem.2017.07.004.

[24] D.V. Vasilyev, Q.J. Shan, Y.T. Lee, V. Soloveva, S.P. Nawoschik, E.J. Kaftan, J. Dunlop, S.C. Mayer, M.R. Bowlby, A novel high-throughput screening assay for HCN channel blocker using membrane potential-sensitive dye and FLIPR, J. Biomol. Screen. 14 (2009) 1119–1128, https://doi.org/10.1177/1087057109345526.

[25] E.R. Benjamin, F. Pruthi, S. Olanrewaju, V.I. Ilyin, G. Crumley, E. Kutlina, K. J. Valenzano, R.M. Woodward, State-dependent compound inhibition of Nav1.2 sodium channels using the FLIPR Vm dye: on-target and off-target effects of diverse pharmacological agents, SLAS Discov. 11 (2006) 29–39, https://doi.org/10.1177/1087057105280918.

[26] S.P. Lee, M.T. Buber, Q. Yang, R. Cerne, R.Y. Cortés, D.G. Sprous, R.W. Bryant, Thymol and related alkyl phenols activate the hTRPA1 channel, Br. J. Pharmacol. 153 (2008) 1739–1749, https://doi.org/10.1038/bjp.2008.85.

[27] M. Finley, J. Cassaday, T. Kreamer, X. Li, K. Solly, G. O'Donnell, M. Clements, A. Converso, S. Cook, C. Daley, R. Kraus, M.-T. Lai, M. Layton, W. Lemaire, D. Staas, J. Wang, Kinetic, analysis of membrane potential dye response to Nav1.7 channel activation identifies antagonists with pharmacological selectivity against NaV1.5, SLAS Discov 21 (2016) 480–489, https://doi.org/10.1177/1087057116629669.

[28] A. Knapman, M. Santiago, Y.P. Du, P.R. Bennallack, M.J. Christie, M. Connor, A continuous, fluorescence-based assay of μ-opioid receptor activation in AtT-20 cells, J. Biomol. Screen. 18 (2013) 269–276, https://doi.org/10.1177/1087057112461376.

[29] R. Fairless, A. Beck, M. Kravchenko, S.K. Williams, U. Wissenbach, R. Diem, A. Cavalié, Membrane potential measurements of isolated neurons using a voltage-sensitive dye, PLOS ONE 8 (2013) e58260, https://doi.org/10.1371/journal.pone.0058260.

[30] K.L. Whiteaker, S.M. Gopalakrishnan, D. Groebe, C.C. Shieh, U. Warrior, D. J. Burns, M.J. Coghlan, V.E. Scott, M. Gopalakrishnan, Validation of FLIPR membrane potential dye for high throughput screening of potassium channel modulators, J. Biomol. Screen. 6 (2001) 305–312, https://doi.org/10.1177/108705710100600504.

[31] A. Yamada, N. Gaja, S. Ohya, K. Muraki, H. Narita, T. Ohwada, Y. Imaizumi, Usefulness and limitation of DiBAC4(3), a voltage-sensitive fluorescent dye, for the measurement of membrane potentials regulated by recombinant large conductance Ca2+-activated K+ channels in HEK293 cells, Jpn. J. Pharmacol. 86 (2001) 342–350, https://doi.org/10.1254/jjp.86.342.

[32] K.R. Konrad, R. Hedrich, The use of voltage-sensitive dyes to monitor signal-induced changes in membrane potential-ABA triggered membrane depolarization in guard cells, Plant J. 55 (2008) 161–173, https://doi.org/10.1111/j.1365-313X.2008.03498.x.

[33] D.F. Baxter, M. Kirk, A.F. Garcia, A. Raimondi, M.H. Holmqvist, K.K. Flint, D. Bojanic, P.S. Distefano, R. Curtis, Y. Xie, A novel membrane potential-sensitive fluorescent dye improves cell-based assays for ion channels, SLAS Discov. 7 (2002) 79–85, https://doi.org/10.1177/108705710200700110.

[34] C. Wolff, B. Fuks, P. Chatelain, Comparative study of membrane potential-sensitive fluorescent probes and their use in ion channel screening assays, J. Biomol. Screen. 8 (2003) 533–543, https://doi.org/10.1177/1087057103257806.

[35] M. Hibino, H. Itoh, K. Kinosita, Time courses of cell electroporation as revealed by submicrosecond imaging of transmembrane potential, Biophys. J. 64 (1993) 1789–1800, https://doi.org/10.1016/S0006-3495(93)81550-9.

[36] K.A. DeBruin, W. Krassowska, Modeling electroporation in a single cell. I. effects Of field strength and rest potential, Biophys. J. 77 (1999) 1213–1224, https://doi.org/10.1016/S0006-3495(99)76973-0.

[37] M. Marty, G. Sersa, J.R. Garbay, J. Gehl, C.G. Collins, M. Snoj, V. Billard, P. F. Geertsen, J.O. Larkin, D. Miklavcic, I. Pavlovic, S.M. Paulin-Kosir, M. Cemazar, N. Morsli, D.M. Soden, Z. Rudolf, C. Robert, G.C. O'Sullivan, L.M. Mir, Electrochemotherapy – an easy, highly effective and safe treatment of cutaneous and subcutaneous metastases: results of ESOPE (European Standard Operating Procedures of Electrochemotherapy) study, Eur. J. Cancer Suppl. 4 (2006) 3–13, https://doi.org/10.1016/j.ejcsup.2006.08.002.

[38] B. Geboers, H.J. Scheffer, P.M. Graybill, A.H. Ruarus, S. Nieuwenhuizen, R.S. Puijk, P.M. van den Tol, R.V. Davalos, B. Rubinsky, T.D. de Gruijl, D. Miklavčič, M. R. Meijerink, High-voltage electrical pulses in oncology: irreversible electroporation, electrochemotherapy, gene electrotransfer, electrofusion, and electroimmunotherapy, Radiology 295 (2020) 254–272, https://doi.org/10.1148/radiol.2020192190.

[39] K.N. Aycock, R.V. Davalos, Irreversible electroporation: background, theory, and review of recent developments in clinical oncology, Bioelectricity 1 (2019) 214–234, https://doi.org/10.1089/bioe.2019.0029.

[40] M. Cemazar, G. Sersa, W. Frey, D. Miklavcic, J. Teissié, Recommendations and requirements for reporting on applications of electric pulse delivery for electroporation of biological samples, Bioelectrochemistry 122 (2018), https://doi.org/10.1016/j.bioelechem.2018.03.005.

[41] T.B. Napotnik, Y.-H. Wu, M.A. Gundersen, D. Miklavčič, P.T. Vernier, Nanosecond electric pulses cause mitochondrial membrane permeabilization in Jurkat cells, Bioelectromagnetics 33 (2012) 257–264, https://doi.org/10.1002/bem.20707.

[42] J. Schindelin, I. Arganda-Carreras, E. Frise, V. Kaynig, M. Longair, T. Pietzsch, S. Preibisch, C. Rueden, S. Saalfeld, B. Schmid, J.-Y. Tinevez, D.J. White, V. Hartenstein, K. Eliceiri, P. Tomancak, A. Cardona, Fiji: an open-source platform for biological-image analysis, Nat. Methods 9 (2012) 676–682, https://doi.org/10.1038/nmeth.2019.

[43] L. Catacuzzeno, B. Fioretti, F. Franciolini, A theoretical study on the role of Ca2+-activated K+ channels in the regulation of hormone-induced Ca2+ oscillations and their synchronization in adjacent cells, J. Theor. Biol. 309 (2012) 103–112, https://doi.org/10.1016/j.jtbi.2012.05.009.

[44] J. Li, H. Lin, Numerical simulation of molecular uptake via electroporation, Bioelectrochemistry 82 (2011) 10–21, https://doi.org/10.1016/j.bioelechem.2011.04.006.

[45] J. Li, W. Tan, M. Yu, H. Lin, The effect of extracellular conductivity on electroporation-mediated molecular delivery, Biochim. Biophys. Acta 2013 (1828) 461–470, https://doi.org/10.1016/j.bbamem.2012.08.014.

[46] J. Li, H. Lin, The current-voltage relation for electropores with conductivity gradients, Biomicrofluidics 4 (2010) 013206, https://doi.org/10.1063/1.3324847.

[47] J.A. Lamas, L. Rueda-Ruzafa, S. Herrera-Pérez, Ion channels and thermosensitivity: TRP, TREK, or both? Int. J. Mol. Sci. 20 (2019) 2371, https://doi.org/10.3390/ijms20102371.

[48] F. Yang, J. Zheng, High temperature sensitivity is intrinsic to voltage-gated potassium channels, eLife 3 (2014) e03255, https://doi.org/10.7554/eLife.03255.

[49] H.G. Glitsch, Electrophysiology of the Sodium-Potassium-ATPase in Cardiac Cells, Physiol. Rev. 81 (2001) 1791–1826, https://doi.org/10.1152/physrev.2001.81.4.1791.

[50] B. Valič, M. Golzio, M. Pavlin, A. Schatz, C. Faurie, B. Gabriel, J. Teissié, M.-P. Rols, D. Miklavčič, Effect of electric field induced transmembrane potential on spheroidal cells: theory and experiment, Eur. Biophys. J. 32 (2003) 519–528, https://doi.org/10.1007/s00249-003-0296-9.

[51] M. Kandušer, M. Šentjurc, D. Miklavčič, Cell membrane fluidity related to electroporation and resealing, Eur. Biophys. J. 35 (2006) 196–204, https://doi.org/10.1007/s00249-005-0021-y.

[52] B. Gabriel, J. Teissié, Control by electrical parameters of short- and long-term cell death resulting from electropermeabilization of Chinese hamster ovary cells, Biochim. Biophys. Acta BBA - Mol. Cell Res. 1266 (1995) 171–178, https://doi.org/10.1016/0167-4889(95)00021-J.

[53] W. Peng, T. Polajžer, C. Yao, D. Miklavčič, Dynamics of cell death due to electroporation using different pulse parameters as revealed by different viability assays, Ann. Biomed. Eng. 52 (2024) 22–35, https://doi.org/10.1007/s10439-023-03309-8.

[54] E.D. Michelakis, G. Sutendra, P. Dromparis, L. Webster, A. Haromy, E. Niven, C. Maguire, T.-L. Gammer, J.R. Mackey, D. Fulton, B. Abdulkarim, M.S. McMurtry, K.C. Petruk, Metabolic modulation of glioblastoma with dichloroacetate, Sci. Transl. Med. 2 (2010), https://doi.org/10.1126/scitranslmed.3000677, 31ra34-31ra34.

[55] T. Ducret, A. Vacher, P. Vacher, Voltage-dependent ionic conductances in the human malignant astrocytoma cell line U87-MG, Mol. Membr. Biol. 20 (2003) 329–343, https://doi.org/10.1080/0968763031000138037.

[56] T. Höfer, Model of intercellular calcium oscillations in hepatocytes: synchronization of heterogeneous cells, Biophys. J. 77 (1999) 1244–1256, https://doi.org/10.1016/S0006-3495(99)76976-6.

[57] L. Catacuzzeno, F. Franciolini, Role of KCa3.1 channels in modulating Ca2+ oscillations during glioblastoma cell migration and invasion, Int. J. Mol. Sci. 19 (2018) 2970, https://doi.org/10.3390/ijms19102970.

[58] N. Gamper, J.D. Stockand, M.S. Shapiro, The use of Chinese hamster ovary (CHO) cells in the study of ion channels, J. Pharmacol. Toxicol. Methods 51 (2005) 177–185, https://doi.org/10.1016/j.vascn.2004.08.008.

[59] A. Varghese, E.M. TenBroek, J. Coles, D.C. Sigg, Endogenous channels in HEK cells and potential roles in HCN ionic current measurements, Prog. Biophys. Mol. Biol. 90 (2006) 26–37, https://doi.org/10.1016/j.pbiomolbio.2005.05.002.

[60] G. Pucihar, T. Kotnik, D. Miklavčič, Measuring the Induced Membrane Voltage with Di-8-ANEPPS, J. vis. Exp. (2009) 1659, https://doi.org/10.3791/1659.

[61] P. Yan, C.D. Acker, W.-L. Zhou, P. Lee, C. Bollensdorff, A. Negrean, J. Lotti, L. Sacconi, S.D. Antic, P. Kohl, H.D. Mansvelder, F.S. Pavone, L.M. Loew, Palette of fluorinated voltage-sensitive hemicyanine dyes, Proc. Natl. Acad. Sci. 109 (2012) 20443–20448, https://doi.org/10.1073/pnas.1214850109.

[62] C.N. Broyles, P. Robinson, M.J. Daniels, Fluorescent, bioluminescent, and optogenetic approaches to study excitable physiology in the single cardiomyocyte, Cells 7 (2018) 51, https://doi.org/10.3390/cells7060051.

[63] K. Trontelj, M. Ušaj, D. Miklavčič, Cell electrofusion visualized with fluorescence microscopy, J. vis. Exp. Jove 2010 (1991), https://doi.org/10.3791/1991.

[64] A.R. Ruiz-Fernández, L. Campos, F. Villanelo, S.E. Gutiérrez-Maldonado, T. Perez-Acle, Exploring the conformational changes induced by nanosecond pulsed electric fields on the voltage sensing domain of a Ca2+ channel, Membranes 11 (2021) 473, https://doi.org/10.3390/membranes11070473.

[65] L. Rems, M.A. Kasimova, I. Testa, L. Delemotte, Pulsed electric fields can create pores in the voltage sensors of voltage-gated ion channels, Biophys. J. 119 (2020) 190–205, https://doi.org/10.1016/j.bpj.2020.05.030.

[66] H.H. Yang, F. St-Pierre, Genetically encoded voltage indicators: opportunities and challenges, J. Neurosci. off. J. Soc. Neurosci. 36 (2016) 9977–9989, https://doi.org/10.1523/JNEUROSCI.1095-16.2016.

[67] L. Catacuzzeno, F. Aiello, B. Fioretti, L. Sforna, E. Castigli, P. Ruggieri, A.M. Tata, A. Calogero, F. Franciolini, Serum-activated K and Cl currents underlay U87-MG glioblastoma cell migration, J. Cell. Physiol. 226 (2011) 1926–1933, https://doi.org/10.1002/jcp.22523.

[68] M.A. Kasimova, E. Lindahl, L. Delemotte, Determining the molecular basis of voltage sensitivity in membrane proteins, J. Gen. Physiol. 150 (2018) 1444–1458, https://doi.org/10.1085/jgp.201812086.

[69] A. Litan, S.A. Langhans, Cancer as a channelopathy: ion channels and pumps in tumor development and progression, Front. Cell. Neurosci. 9 (2015) 86, https://doi.org/10.3389/fncel.2015.00086.

[70] H.J. Gould, D. Paul, Cancer as a channelopathy—appreciation of complimentary pathways provides a different perspective for developing treatments, Cancers 14 (2022) 4627, https://doi.org/10.3390/cancers14194627.

[71] J. Mathews, F. Kuchling, D. Baez-Nieto, M. Diberardinis, J.Q. Pan, M. Levin, Ion channel drugs suppress cancer phenotype in NG108-15 and U87 Cells: toward novel electroceuticals for glioblastoma, Cancers 14 (2022) 1499, https://doi.org/10.3390/cancers14061499.
[72] E.P.W. Jenkins, A. Finch, M. Gerigk, I.F. Triantis, C. Watts, G.G. Malliaras, Electrotherapies for glioblastoma, Adv. Sci. 8 (2021) 2100978, https://doi.org/10.1002/advs.202100978.
[73] D. Miklavčič, G. Serša, M. Kryžanowski, S. Novakovič, F. Bobanović, R. Golouh, L. Vodovnik, Tumor treatment by direct electric current-tumor temperature and pH, electrode material and configuration, Bioelectrochem. Bioenerg. 30 (1993) 209–220, https://doi.org/10.1016/0302-4598(93)80080-E.